Effect of intercritical temperature on quenching and partitioning steels originated from martensitic pre-microstructure

Ran Ding, Di Tang, and Aimin Zhao[a)]
Engineering Research Institute, University of Science and Technology Beijing, Beijing 100083, People's Republic of China; Beijing Laboratory of Metallic Materials and Processing for Modern Transportation, Beijing 100083, People's Republic of China; and National Engineering Research Center of Advanced Rolling, Beijing 100083, People's Republic of China

Rui Dong, Junye Cheng, and Xiang Meng
Engineering Research Institute, University of Science and Technology Beijing, Beijing 100083, People's Republic of China

(Received 19 April 2014; accepted 4 September 2014)

The effect of the intercritical temperature on the microstructure and mechanical properties of a newly developed quenching and partitioning steel using martensitic microstructure prior to the heat treatment process was studied. Such a quenching and partitioning process possessed a unique microstructure evolution, especially during intercritical annealing after prequenching. Excellent mechanical properties were obtained due to this unique multiphase microstructure. Significant amount of interlath-retained austenite was acquired and the relationship between the microstructure and work-hardening behaviors was proposed. The martensite/austenite islands increased at elevated annealing temperature, which deteriorated the total elongation and increased the tensile strength as hard constituents when it was excessive. The result indicated that the present full martensitic microstructure before the intercritical annealing is probably more suitable to an industrial application and is a better way to produce high strength steels with suitable ductility.

I. INTRODUCTION

In the past few years, the automobile industry has an increasing demand to the development of new advanced high strength steels (AHSS) to manufacture weight-reduced, environment friendly and fuel efficient vehicles. Multiphase steels were put forward to be ideal solutions that cater to these demands, such as dual-phase (DP)[1] and transformation-induced plasticity (TRIP) steels.[2] A new heat treatment process known as "quenching and partitioning" (Q&P) has been shown to be a superb processing option for the production of high strength steels with significant amounts of retained austenite,[3–5] and has been assessed as a potential solution to provide excellent strength/ductility combinations in high strength steels. Although autobody application represented the first implementation of Q&P on an industrial scale, this heat treatment is also applicable to a range of other potential applications.[6]

In general, a Q&P process includes quenching from full austenization or intercritical region and partitioning at the quenching temperature between the martensite start temperature (M_s) and the martensite finish temperature (M_f) or above M_s temperature.[3–7] Generally, a ferrite plus pearlite initial microstructure is used prior to the Q&P process. However, mechanical properties after the Q&P process significantly depend on the original microstructure prior to the Q&P process regardless of the heat treatment conditions. Therefore, the resulting microstructure and mechanical properties after using different original microstructures prior to the Q&P process are very appealing. On the research by Santofimia et al.,[8] on increasing the Mn content to 3.5 wt%, the initial microstructures after hot rolling and air cooling consisted of martensite and polygonal ferrite. The application of Q&P heat treatments to such microstructures had resulted in good mechanical property compared with current commercial AHSS steels.

In this study, by combining prequenching, Q&P procedures, a new type of Q&P steels (QQP steels) using a fully martensitic microstructure prior to the Q&P process was developed, and its unique multiphase microstructure and novel mechanical properties were studied.

II. MATERIAL AND METHODS

A. Composition design

The chemical composition of the investigated material is given in Table I. Carbon and manganese are important elements in stabilizing the retained austenite. The addition

[a)]Address all correspondence to this author.
e-mail: aimin.zhao@ustb.edu.cn
DOI: 10.1557/jmr.2014.285

 © Materials Research Society 2014

https://doi.org/10.1557/jmr.2014.285 Published online by Cambridge University Press

of manganese was favorable to lower the transformation temperatures such as A_{C1}, A_{C3}, M_s, and M_f; thus austenitization could be carried out at relatively low temperatures leading to the refinement of austenite and martensite packets. Furthermore, the formation of bainite was delayed. Silicon was added to hinder the precipitation of carbide, which could dilute the carbon enrichment of austenite in the partitioning progress.

B. Rolling and heat treatment

After 50 kg vacuum melting, the ingots were forged to 40 mm in thickness, and hot rolled to 5 mm in thickness, with the final rolling temperature of 870 °C and coiling at 660 °C for 1 h, and then air cooled. Sheets of 1.5 mm thickness were produced by cold rolling, followed by heating to 900 °C for 15 min and quenching to obtain a completely martensitic structure.

When annealed at the $(A_{C1} + A_{C3})/2$ temperature, a high fraction of retained austenite and excellent mechanical properties can be expected to be achieved in TRIP steels.[9] To select appropriate intercritical annealing temperatures, the A_{C1} and A_{C3} temperatures corresponding to the heating rate of 5 °C/s for the annealing of fully martensitic microstructure were measured by dilatometry as shown in Fig. 1(a). The A_{C1} and A_{C3} were estimated to be 697 and 853 °C respectively, so the suitable intercritical annealing temperature is around 775 °C. Therefore, the intercritical annealing temperatures in this study were chosen to be 760, 780, and 800 °C. The samples were known as QQP-760, QQP-780, and QQP-800 respectively. The intercritical annealing outlined in Fig. 1(b) was conducted using 1.5 × 70 × 220 mm samples in a CCT-AY-II (ULVAC-RIKO) simulator.

TABLE I. The chemical composition in mass% of the investigated steel.

C	Si	Mn	P	S	Fe
0.20	1.63	2.01	0.0079	0.0045	Balance

C. Sample preparation

Nital and LePera etching were used to distinguish each constituent of the samples. The microstructure morphology and phase distribution were subsequently observed with ZEISS AX10 optical microscope (OM; Göttingen, Lower Saxony, Germany) and ZEISS ULTRA 55-type field emission scanning electron microscope (FE-SEM; Oberkochen, Baden-Württemberg, Germany). Transmission electron microscopy (TEM) was performed by using Tecnai G2 F30 S-TWIN-type transmission electron microscope (Hillsboro, OR) and TEM samples were obtained by punching from the same region of the specimens, and then followed by double-jet thinning in the electrolyte of 5% perchloric acid and 95% glacial acetic acid, as the voltage was 20 V and the temperature −20 °C.

Electron back scattering patterns (EBSD) equipped in FE-SEM were performed and the acquired data were processed with Channel 5 software provided by Oxford HKL Technology. X-ray diffraction (XRD) tests were made by using Cu K_α radiation. The retained austenite volume fraction was determined by using the integrated intensity of the $(200)_\gamma$, $(220)_\gamma$, $(311)_\gamma$, $(200)_\alpha$, and $(211)_\alpha$ peaks.[10] Samples for EBSD and XRD were ground and electrolytically polished in the electrolyte of 20% perchloric acid and 80% ethanol at 15 V for 25 s.

The tensile test samples were machined into dog-bone geometry and the gauge length was 50 mm with the crosshead speed at 2 mm/min. The measured data were converted into true stress and true strain. Strain-hardening behaviors were characterized by the work-hardening rate n,[11] calculated from the true stress–strain curves as:

$$n = d\ln\sigma/d\ln\varepsilon$$

with σ, the true strain, and ε, the true stress.

III. RESULTS AND DISCUSSION

A. As received microstructure

As shown in Fig. 2(a), after hot rolling and coiling at 660 °C for 1 h, the investigated material appeared to

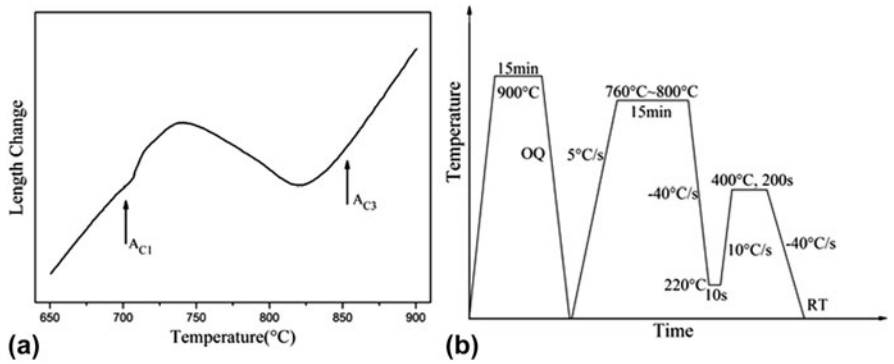


FIG. 1. (a) Dilatometry curve corresponding to the heating rate of 5 °C/s for annealing from the quenched condition; (b) the illustration of the heat treatments of QQP steels.

https://doi.org/10.1557/jmr.2014.285 Published online by Cambridge University Press

have a traditional ferrite–pearlite structure. This would be helpful in acquiring a large cold-rolling reduction. A fibrous structure was obtained after cold rolling with a reduction of 70% which would raise the nucleation rate of austenite during austenization to refine the microstructure before quenching.

B. Quenched and intercritical microstructure

A fully martensitic microstructure was obtained after oil quenching from 900 °C holding for 15 min as shown in Figs. 3(a) and 4(a) with nital etching. Samples for observing the corresponding intercritical microstructures were prepared by quenching from each ending of the intercritical annealing and the OM micrographs were shown in Figs. 3(b)–3(d). After LePera etching, the martensite and retained austenite (representing the intercritical austenite) appear white while the ferrite appears dark yellow.[12] As a result, two morphologies of the austenite existed in low alloyed steels when annealing the martensitic structure in the intercritical region, i.e., acicular austenite (γ_a) and blocky austenite (γ_b). γ_a was formed between the martensite lath boundaries while γ_b was mainly embedded in prior austenite grain boundaries and a small proportion of it formed in packet boundaries of lath martensite at a relatively high temperature.[13] As the annealing temperature rose, γ_b coarsened

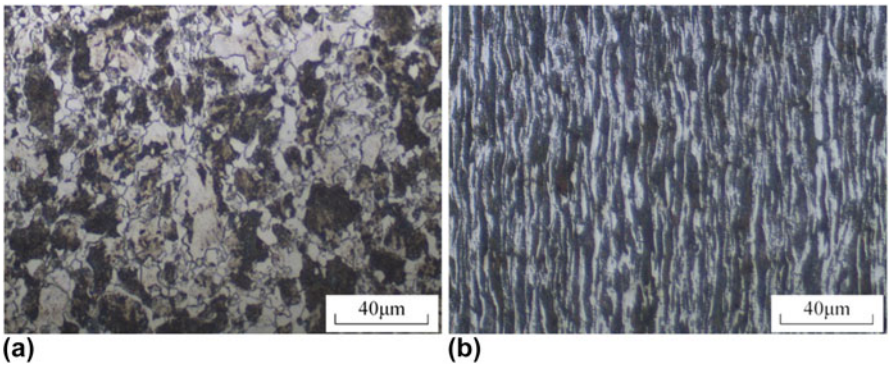


FIG. 2. Optical micrographs of the microstructures of (a) hot-rolled condition and (b) cold-rolled condition.

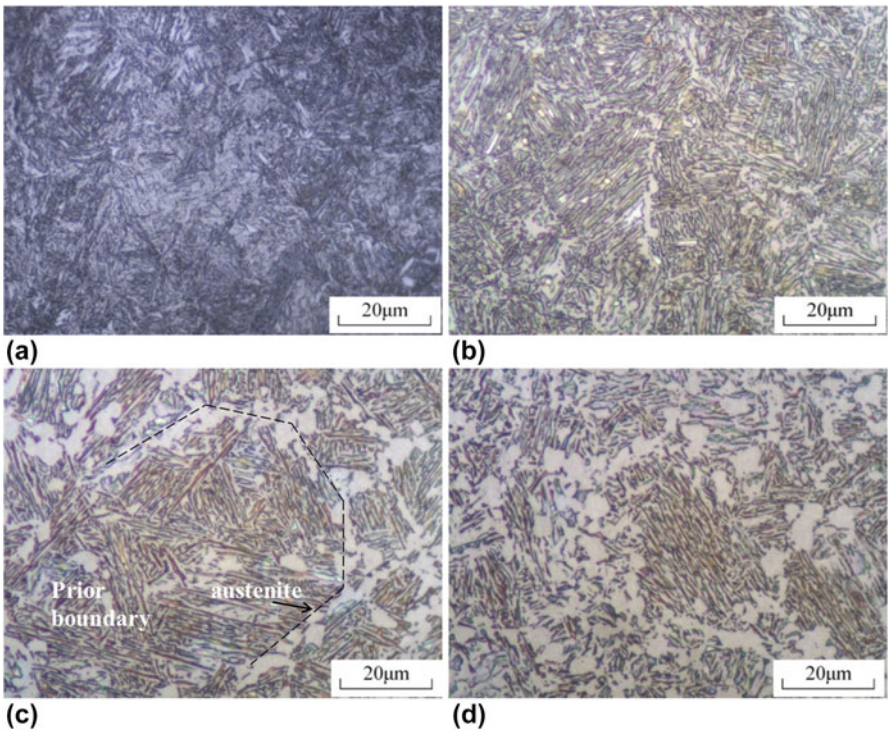


FIG. 3. Optical micrographs of the microstructures of (a) quenched condition, direct quenching condition after annealing at (b) 760 °C, (c) 780 °C, and (d) 800 °C with LePera etching, where the white region represents martensite or retained austenite and the tawny region represents ferrite with prior martensitic lath morphology.

https://doi.org/10.1557/jmr.2014.285 Published online by Cambridge University Press

and became the majority in the intercritical microstructure, whereas the coarsening of γ_a was less obvious as shown in Figs. 3(b)–3(d). No polygonal ferrite was found in each sample, indicating that the recrystallization and nucleation of the α-phase barely existed during the short time annealing. A sufficient amount of alloying elements was responsible for the suppression of the recrystallization of martensite, so the lath-like morphology was partly preserved except for the portion occupied by γ_b.

The formation of the intercritical austenite that started with the growth of prior retained austenite always has a preferential orientation.[13,14] γ_a emerges mainly from the growth of austenite preserved during the prequenching process between martensite laths and is Kurdjumov–Sachs related to the laths nearby; while there is no austenite retained in prior austenite grain boundaries, γ_b nucleated from dissolved/undissolved carbide or regions with higher carbon content and has an independent orientation.

C. Resulting microstructure

The final microstructures after the Q&P process are shown in Figs. 4(b)–4(d). Compared with the quenching microstructure, the lath-like morphology was preserved to some extent after the Q&P process at 760 °C. As the annealing temperature elevated, the islands which were γ_b in the intercritical region increased and were composed of martensite and retained austenite (M/A) in the final microstructure after annealing at 780 and 800 °C. Therefore, the lath-like morphology was undermined at the relatively high temperature. As shown in Fig. 4(d), the lath-like morphology had almost disappeared due to the large area occupied by M/A islands.

Heating the martensitic microstructure in the intercritical region would lead to a fast recovery of martensite. The instability of cementite then produces a stable austenite highly enriched in carbon. Because no deformation was applied to the martensitic microstructure before annealing and because of the relatively low dislocation density due to the chemical composition,[15–17] the recrystallization of martensite hardly occurred, which is consistent with the result in sub Sec. III. A. The migration of lath boundaries might exist while annealing, but it is not evident merely from the SEM micrographs and not the focal point of this study. Moreover, there are no precipitates observed both in the SEM and TEM microscopies.

D. Microstructure evolution

The TEM micrograph of QQP-780 is shown in Fig. 5. Interlath austenite, fresh martensite transformed from γ_a are indicated with arrows. After partitioning and cooling to room temperature, some γ_a partly transformed to fresh martensite, and the rest preserved as interlath-retained austenite. It is more convincing in the enlargement of section A in Fig. 7(b) as shown in Fig. 8(c) that one γ_a lath was divided into two phases between the α-phase laths. It is proposed that such location of interlath-retained austenite facilitated carbon enrichment by itself due to the increasing diffusion paths because of relatively high dislocation density acting as a rapid diffusion channel, and the inherent short lath morphology in one dimension.

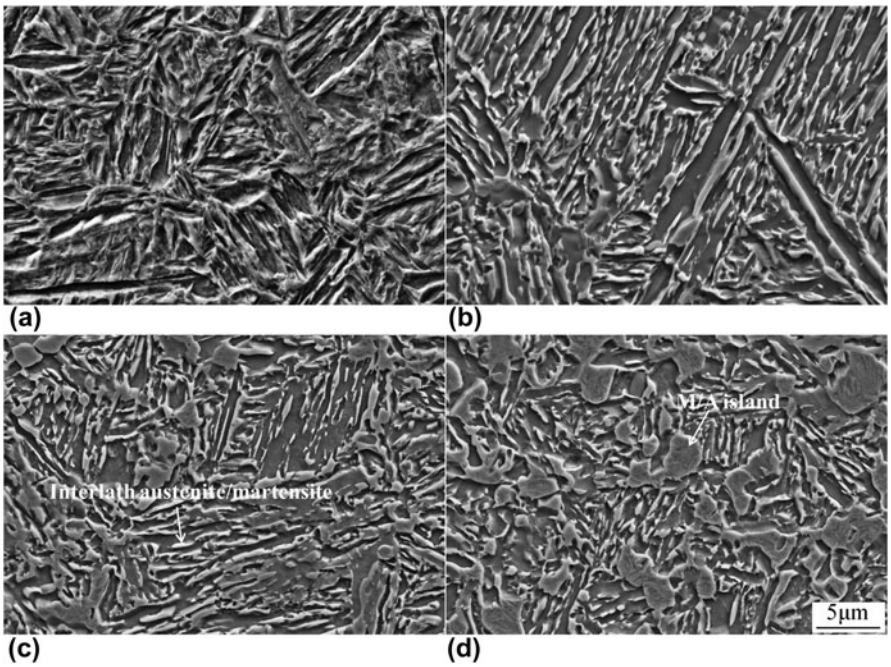


FIG. 4. SEM micrographs of the microstructures of (a) quenched condition, final condition after annealing at (b) 760 °C, (c) 780 °C, and (d) 800 °C.

https://doi.org/10.1557/jmr.2014.285 Published online by Cambridge University Press

Moreover, it is proposed that surrounded by α-phase laths the stability of the interlath-retained austenite was further improved by increasing the three-dimensional compressive stress.[18]

E. Mechanical properties

As shown in Fig. 6 and Table II, the new type of Q&P steels exhibited eminent mechanical properties when annealing at 780 and 800 °C. The yield strength rose as the annealing temperature went up, and a superior total elongation and product with strength and ductility were obtained by annealing at 780 °C, with the higher content of the retained austenite. After annealing at 800 °C, almost the same retained austenite content led to the mechanical properties which were not as good as the sample annealing at 780 °C. The reason was proposed to be the redundant M/A islands which were hard constituents producing an increasing yield strength and a decreasing elongation.[19] The relatively low total elongation of QQP-760 is proposed to be associated with the comparatively low content of retained austenite.

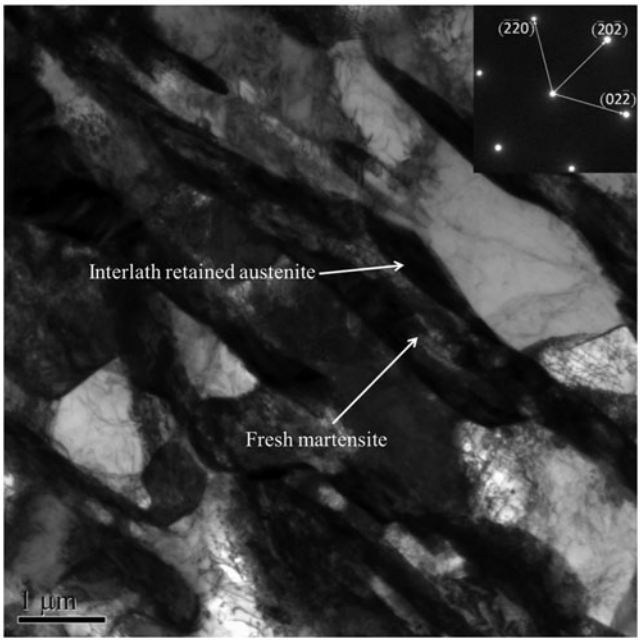


FIG. 5. TEM micrographs of QQP-780 and the electron diffraction pattern of the interlath-retained austenite.

The work-hardening rate n as a function of the true strain is shown as Fig. 6(b). The straight line corresponds to the instability criterion $n = \varepsilon_u$, where ε_u is the true strain at the beginning of necking. On annealing at different temperatures, various work-hardening behaviors were observed. After annealing at 760 °C, the initial n increased rapidly up to 0.35 at the early stage of the deformation. This phenomenon is very similar to the work-hardening behavior of DP steels,[20] which can effectively improve the uniformity of the strain distribution, and delay plastic instabilities during the application of DP steels in the automotive stamping.[21] Moreover, QQP-760 also had a low yield ratio as shown in Table II. It is proposed that a well-shaped and fibrous microstructure led to the similarity to DP steels. The n decreased gradually as the deformation carried on till necking due to the insufficient volume fraction of the retained austenite. Work-hardening behaviors of QQP-780 and QQP-800 are very different compared with that of QQP-760, which revealed a strong persistent work hardening. The n was maintained between 0.20 and 0.25 during most part of the deformation and it was attributed to the TRIP effect of the retained austenite.

1. EBSD analysis

Typical EBSD analysis results of the QQP steels' intercritical annealing at 780 °C are shown in Fig. 7

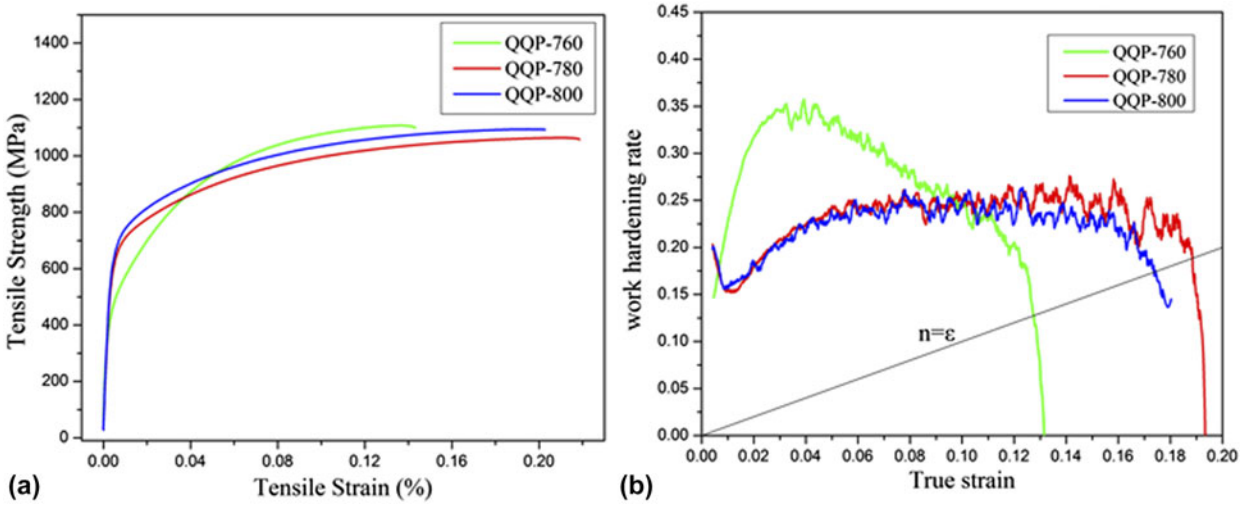


FIG. 6. (a) Stress–strain curves of QQP samples at room temperature and (b) corresponding work-hardening rate-true strain curves of different specimens.

https://doi.org/10.1557/jmr.2014.285 Published online by Cambridge University Press

after being processed with the Channel 5 EBSD software. Austenite is revealed in blue as shown in Fig. 7(b). A considerable amount of interlath austenite was obtained under suitable annealing conditions, and it is thought to be a key constituent that is beneficial to the enhancement of mechanical properties by efficaciously relieving the stress concentration between laths and it is well known that films of retained austenite are better able to resist strain-induced martensitic transformation than any coarser-retained austenite.[18,22–24] In addition to the results already proposed in Sec. III. C, interlath-retained austenite is able to decrease the effective fracture grain size, and thus helps to blunt propagating microcracks,[25] and the small size of the retained austenite itself also acts as a stabilizing factor.[26,27]

The dark regions represent the M/A islands because of their high defect densities and large quantities of substructures that resulted in low qualities of Kikuchi bands.[28]

TABLE II. Mechanical properties of investigated steels, where YS is the yield strength, YR is the yield ratio, UTS is the ultimate tensile strength, TEL is the total elongation of each sample, and f_{RA} is the volume fraction of the retained austenite obtained from XRD tests.

Sample	YS (MPa)	YR	UTS (MPa)	TEL (%)	UTS·TEL (MPa %)	f_{RA} (%)
QQP-760	445	0.40	1108	16.68	18,481	8.93
QQP-780	517	0.48	1074	25.08	26,685	12.42
QQP-800	650	0.59	1095	23.26	25,470	12.26

According to the research by Hara et al.,[13] γ_a was formed mainly by the growth of austenite preserved during the prequenching process. Therefore, interlath austenite that originated from the same prior austenite possessed the same crystal orientation.[8] After the Q&P process, γ_a was partly preserved in the form of interlath-retained austenite because of carbon enrichment. Thus, as shown in Fig. 7(d), the picture can be roughly divided into three regions in accordance with the same color that retained austenite displays. The M/A islands and retained austenite of independent color located near the dividing line confirm that it may be the prior austenite boundaries.

The enlargement of section B in Fig. 7(b) is shown as Fig. 8(a). The yellow and black lines in the enlarged orientation maps represent phase boundaries with the Kurdjumov–Sachs orientation relationship between α-phase and γ-phase in a tolerance of 2° and the boundaries beyond 5° deviation from the specified lattice correlation, respectively. Although the crystal orientation of martensite varied during the heat treatment after quenching, a strong orientation relationship still existed between the ferrite laths and the interlath-retained austenite. Surrounded by α-phase laths, which almost have the same crystal orientation as shown in Fig. 7(c), the boundary is nearly Kurdjumov–Sachs related at all parts.

The enlargement of section C in Fig. 7(b) is shown as Fig. 8(b). The different color of the retained austenite indicates that it does not belong to any of the three prior

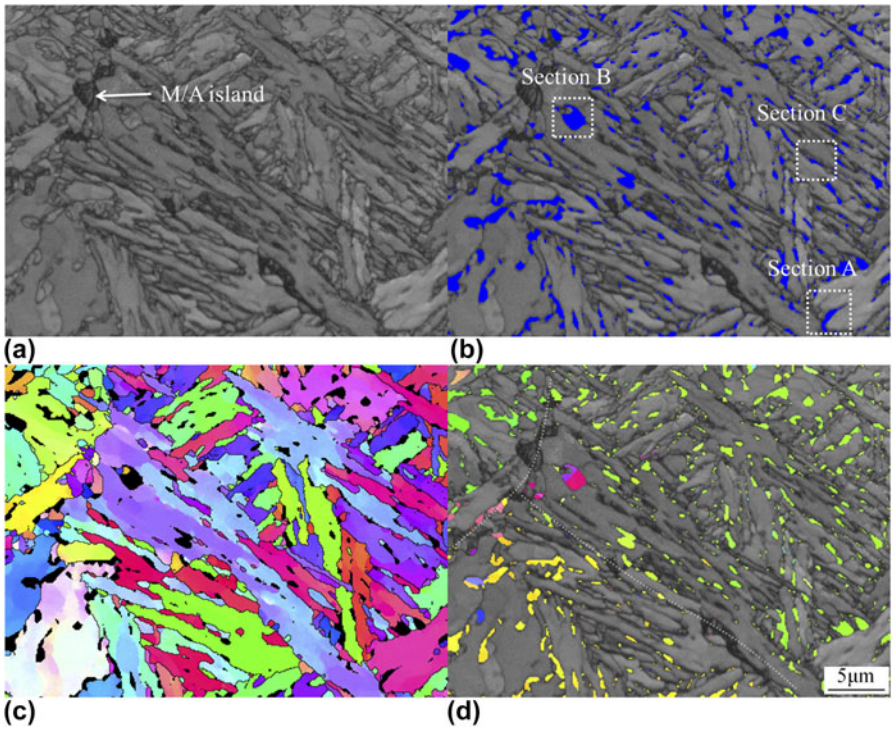


FIG. 7. EBSD microstructures of QQP-780, (a) image quality map, (b) image quality map with the blue regions representing the retained austenite, (c) inverse pole map of BCC, and (d) inverse pole map of FCC.

https://doi.org/10.1557/jmr.2014.285 Published online by Cambridge University Press

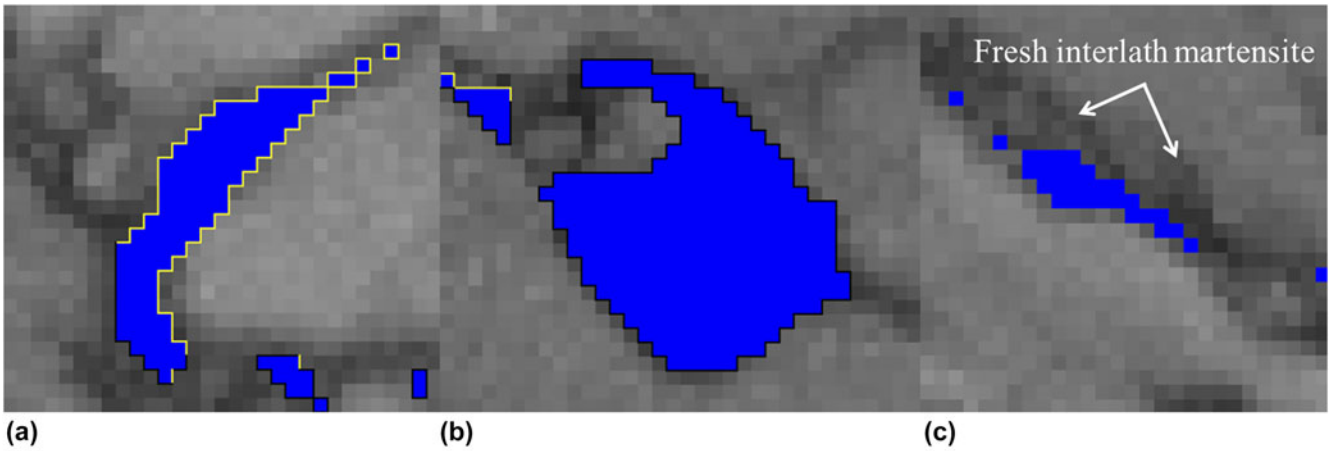


FIG. 8. The enlargements of (a) section A and (b) section B with Kurdjumov–Sachs relationship reflected by yellow lines, while the boundaries beyond 5° deviation from Kurdjumov–Sachs relationship reflected by black lines and (c) section C.

austenite regions as shown in Fig. 7(d); i.e., it is a new austenite that nucleated and grew up during annealing. As it is in a pretty close location to the prior austenite boundary and blocky morphology, it is thought to be γ_b partly preserved because of carbon enrichment in the partitioning process. No Kurdjumov–Sachs relationships exist at the grain boundaries which confirms that it did not originate from the austenite preserved after prequenching.

The retained austenite is a critical constitution in Q&P steels and parameters such as its volume fraction, size, chemical composition, morphology, location and stress distribution are the well-known factors affecting its stability. Three effects of the retained austenite on the ductility have been proposed already. One is the TRIP effect, which involves relaxing the local stress concentration by the martensitic transformation.[29] The other is the blocking microcrack propagation (BMP) effect.[30] The last is the dislocation absorption by the retained austenite (DARA) effect observed in high strength Q–P–T steels.[31] As shown in Fig. 7(d), most retained austenite is of the interlath kind, which confirms that it is more thermally stable during cooling to the room temperature as proposed in Sec. III. C.

The microstructure of QQP steel is a little similar to that of conventional Q&P steels which are fully austenitized[32] and the matrix is mainly (recovered) martensite formed during the quenching just before the partitioning process. Instead of being constituted by martensite plus retained austenite, QQP steel possesses multiple constitution of the recovered α-phase with previous lath morphology, M/A islands, blocky, and interlath-retained austenite. Such a multiphase microstructure had shown excellent mechanical properties during deformation. When compared with conventional Q&P steels quenching from the intercritical region, polygonal ferrite barely existed in QQP steel, but its elongation was not deteriorated. Moreover, the harder the matrix, the smaller the mean-stress level in the austenite,[33,34] which enhanced the stability of the retained austenite and delayed strain-induced martensitic transformation. Therefore, martensitic islands could be treated as strengthening particles that improved the strength of the matrix, and moreover, produced a "shielding" effect that decreased the austenite transformation rate.[26] However, excessive M/A islands could deteriorate the elongation due to the improperness that still treated them as secondary particles because of their increasing proportion.

During further research, we had raised the carbon content up to 0.28 wt% and investigated the effect on this kind of heat treatment. Similar microstructures and the same optimal annealing temperature have been observed. The total volume fraction of the retained austenite of 14.8%, tensile strength of 1280 MPa and total elongation of 23.6% were obtained, which indicated that the possible steel grade of this process could exceed 1300 MPa with suitable ductility and could be used in the automobile industry and other mechanical applications including, but not limited to, a sheet shape. For example, such a heat treatment could be used in steel rods and wires to improve their performance. The proposed process is similar to the Q&P process but the microstructure evolution is quite different indeed, especially during the intercritical annealing. As a result of martensitic pre-microstructure, excellent mechanical properties were achieved compared with the conventional Q&P steel, which indicated that the present full martensitic microstructure before the intercritical annealing is probably more suitable to an industrial application, especially for steels with high hardenability which could obtain full martensitic microstructure without controlled cooling. That is, after the finish rolling, steels could be air cooled (high hardenability) or fast cooled (low hardenability) to obtain the martensitic microstructure, and then annealed with continuous annealing lines.

https://doi.org/10.1557/jmr.2014.285 Published online by Cambridge University Press

IV. CONCLUSIONS

In this study, the combination of prequenching and Q&P procedures resulted in a new type of Q&P steels, which possessed excellent mechanical properties. Its disparate multiphase microstructure has been studied and the effects of annealing temperatures on the final microstructure and mechanical properties have been revealed. A considerable amount of interlath-retained austenite has been proposed to be a key constituent that played an important role in the good work-hardening behaviors of QQP steels.

ACKNOWLEDGMENTS

This research was supported by the National Natural Science Foundation of China (Grant Nos. 51271035 and 51371032).

REFERENCES

1. A. Kumar, S.B. Singh, and K.K. Ray: Influence of bainite/martensite-content on the tensile properties of low carbon dual-phase steels. *Mater. Sci. Eng., A* **474**(1), 270 (2008).
2. S. Zaefferer, J. Ohlert, and W. Bleck: A study of microstructure, transformation mechanisms and correlation between microstructure and mechanical properties of a low alloyed TRIP steel. *Acta Mater.* **52**(9), 2765 (2004).
3. D.V. Edmonds, K. He, F.C. Rizzo, B.C. De Cooman, D.K. Matlock, and J.G. Speer: Quenching and partitioning martensite—A novel steel heat treatment. *Mater. Sci. Eng., A* **438**, 25 (2006).
4. J.G. Speer, D.K. Matlock, B.C. De Cooman, and J.G. Schroth: Carbon partitioning into austenite after martensite transformation. *Acta Mater.* **51**(9), 2611 (2003).
5. L. Xu, Z. Yan, Y. Liu, H. Li, B. Ning, and Z. Qiao: Microstructure evolution and martensitic transformation behaviors of 9Cr–1.8 W–0.3 Mo ferritic heat-resistant steel during quenching and partitioning treatment. *J. Mater. Res.* **28**(20), 2835 (2013).
6. J. Tobata, K.L. Ngo-Huynh, N. Nakada, T. Tsuchiyama, and S. Takaki: Role of silicon in quenching and partitioning treatment of low-carbon martensitic stainless steel. *ISIJ Int.* **52**(7), 1377 (2012).
7. X.D. Wang, N. Zhong, Y.H. Rong, T.Y. Hsu, and L. Wang: Novel ultrahigh-strength nanolath martensitic steel by quenching-partitioning-tempering process. *J. Mater. Res.* **24**(1), 260 (2009).
8. M.J. Santofimia, T. Nguyen-Minh, L. Zhao, R. Petrov, I. Sabirov, and J. Sietsma: New low carbon Q&P steels containing film-like intercritical ferrite. *Mater. Sci. Eng., A* **527**(23), 6429 (2010).
9. O. Matsumura, Y. Sakuma, and H. Takechi: Enhancement of elongation by retained austenite in intercritical annealed 0.4 C-1.5 Si-0.8 Mn steel. *Trans. Iron Steel Inst. Jpn.* **27**(7), 570 (1987).
10. B.D. Cullity and S.R. Stock: *Elements of X-ray Diffraction*, Vol. **3** (Prentice Hall, New York, 2001), p. 484.
11. P. Jacques, F. Delannay, X. Cornet, P. Harlet, and J. Ladriere: Enhancement of the mechanical properties of a low-carbon, low-silicon steel by formation of a multiphased microstructure containing retained austenite. *Metall. Mater. Trans. A* **32**(11), 2759 (2001).
12. F.S. Lepera: Improved etching technique for the determination of percent martensite in high-strength dual-phase steels. *Metallography* **12**(3), 263 (1979).
13. T. Hara, N. Maruyama, Y. Shinohara, H. Asahi, G. Shigesato, M. Sugiyama, and T. Koseki: Abnormal α to γ transformation behavior of steels with a martensite and bainite microstructure at a slow reheating rate. *ISIJ Int.* **49**(11), 1792 (2009).
14. N.C. Law and D.V. Edmonds: The formation of austenite in a low-alloy steel. *Metall. Mater. Trans. A* **11**(1), 33 (1980).
15. T. Tsuchiyama, Y. Miyamoto, and S. Takaki: Recrystallization of lath martensite with bulge nucleation and growth mechanism. *ISIJ Int.* **41**(9), 1047 (2001).
16. A. Galibois and A. Dube: Recrystallization kinetics of martensitic extra-low carbon steels. *Can. Metall. Q.* **3**(4), 321 (1964).
17. M. Natori, Y. Futamura, T. Tsuchiyama, and S. Takaki: Difference in recrystallization behavior between lath martensite and deformed ferrite in ultralow carbon steel. *Scr. Mater.* **53**(5), 603 (2005).
18. A.S. Podder, I. Lonardelli, A. Molinari, and H.K.D.H. Bhadeshia: Thermal stability of retained austenite in bainitic steel: An in situ study. *Proc. R. Soc. A* **467**(2135), 3141 (2011).
19. H. Ikawa, H. Oshige, and T. Tanoue: Effect of martensite-austenite constituent on HAZ toughness of a high strength steel. *Trans. Jpn. Weld. Soc.* **11**(2), 87 (1980).
20. L.F. Ramos, D.K. Matlock, and G. Krauss: On the deformation behavior of dual-phase steels. *Metall. Mater. Trans. A* **10**(2), 259 (1979).
21. G. Ingarao, R.D. Lorenzo, and F. Micari: Analysis of stamping performances of dual phase steels: A multi-objective approach to reduce springback and thinning failure. *Mater. Des.* **30**(10), 4421 (2009).
22. H.K.D.H. Bhadeshia and D.V. Edmonds: Bainite in silicon steels: New composition–property approach. Part 1. *Met. Sci.* **17**(9), 411 (1983).
23. H.K.D.H. Bhadeshia and D.V. Edmonds: Bainite in silicon steels: New composition–property approach. Part 2. *Met. Sci.* **17**(9), 420 (1983).
24. H.K.D.H. Bhadeshia and A.R. Waugh: Bainite: An atom-probe study of the incomplete reaction phenomenon. *Acta Metall.* **30**(4), 775 (1982).
25. V.T.T. Miihkinen and D.V. Edmonds: Fracture toughness of two experimental high-strength bainitic low-alloy steels containing silicon. *Mater. Sci. Technol.* **3**(6), 441 (1987).
26. P.J. Jacques, F. Delannay, and J. Ladrière: On the influence of interactions between phases on the mechanical stability of retained austenite in transformation-induced plasticity multiphase steels. *Metall. Mater. Trans. A* **32**(11), 2759 (2001).
27. S. Lee, S.J. Lee, and B.C. De Cooman: Austenite stability of ultrafine-grained transformation-induced plasticity steel with Mn partitioning. *Scr. Mater.* **65**(3), 225 (2011).
28. M.J. Santofimia, L. Zhao, R. Petrov, and J. Sietsma: Characterization of the microstructure obtained by the quenching and partitioning process in a low-carbon steel. *Mater. Charact.* **59**(12), 1758 (2008).
29. S. Chatterjee, H.S. Wang, J.R. Yang, and H.K.D.H. Bhadeshia: Mechanical stabilisation of austenite. *Mater. Sci. Technol.* **22**(6), 641 (2006).
30. C.G. Lee, S.J. Kim, T.H. Lee, and S. Lee: Effects of volume fraction and stability of retained austenite on formability in a 0.1 C–1.5 Si–1.5 Mn–0.5 Cu TRIP-aided cold-rolled steel sheet. *Mater. Sci. Eng., A* **371**(1), 16 (2004).

https://doi.org/10.1557/jmr.2014.285 Published online by Cambridge University Press

31. K. Zhang, M. Zhang, Z. Guo, N. Chen, and Y. Rong: A new effect of retained austenite on ductility enhancement in high-strength quenching–partitioning–tempering martensitic steel. *Mater. Sci. Eng., A* **528**(29), 8486 (2011).
32. D.V. Edmonds, K. He, M.K. Miller, F.C. Rizzo, A.J. Clarke, D.K. Matlock, and J.G. Speer: Microstructural features of 'quenching and partitioning': A new martensitic steel heat treatment. *Mater. Sci. Forum* **539**, 4819 (2007).
33. A.G. Evans, J.W. Hutchinson, and R.M. McMeeking: Stress–strain behavior of metal matrix composites with discontinuous reinforcements. *Scr. Metall. Mater.* **25**(1), 3 (1991).
34. G. Bao, J.W. Hutchinson, and R.M. McMeeking: The flow stress of dual-phase, non-hardening solids. *Mech. Mater.* **12**(2), 85 (1991).

https://doi.org/10.1557/jmr.2014.285 Published online by Cambridge University Press